

2

UCRL- 84477  
PREPRINT

CONF-801037--11

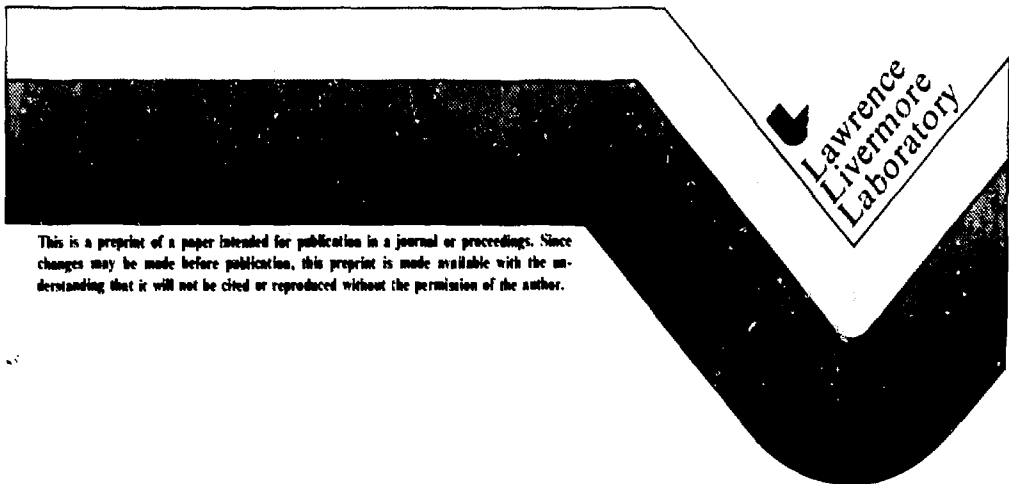
INTERFEROMETRIC MEASUREMENTS OF MULTILAYER  
AND DOUBLE SHELL INERTIAL FUSION TARGETS

**MASTER**

B. W. Weinstein  
J. T. Weir  
D. L. Willenborg

This paper was prepared for submission to the  
27th National American Vacuum Society Symposium  
Detroit, Michigan  
October 14-17, 1980

August 26, 1980



This is a preprint of a paper intended for publication in a journal or proceedings. Since changes may be made before publication, this preprint is made available with the understanding that it will not be cited or reproduced without the permission of the author.

INTERFEROMETRIC MEASUREMENTS OF MULTILAYER  
AND DOUBLE-SHELL INERTIAL FUSION TARGETS\*

B. W. Weinstein, J. T. Weir and D. L. Willenborg,

Lawrence Livermore National Laboratory,

P. O. Box 5508

Livermore, California 94550

ABSTRACT

Optical interference microscopy plays an important role in the measurement of targets for inertial confinement fusion experiments. We describe how these techniques are applied to the measurement of thickness and refractive index of multilayer films on both flat substrates and microsphere targets. We also discuss procedures for manipulating and examining microsphere targets to measure surface defects and wall thickness variations anywhere on the target. Finally, we describe the use of optical interferometry to measure the individual components and final assembled structure of double-shell targets. The accuracy of these measurements is from 0.03 to 0.5  $\mu\text{m}$ , depending on the specific application.

\*Work performed under the auspices of the U.S. Department of Energy by the Lawrence Livermore National Laboratory under contract number W-7405-ENG-48.

**DISCLAIMER**

This book was prepared as an account of work sponsored by an agency of the United States Government. Neither the United States Government nor any agency thereof, nor any of their employees, makes any warranty, express or implied, or assumes any legal liability or responsibility for the accuracy, completeness, or usefulness of any information, apparatus, product, or process disclosed, or represents that its use would result in infringement of privately owned rights. Reference herein to any specific commercial product, process, or service by trade name, trademark, manufacturer, or otherwise, does not necessarily constitute or imply its endorsement, recommendation, or favoring by the United States Government or any agency thereof. The views and opinions of authors expressed herein do not necessarily state or reflect those of the United States Government or any agency thereof.

DISTRIBUTION OF THIS DOCUMENT IS UNLIMITED

Inertial confinement fusion (ICF) experiments use as targets various polymer and metal films and hollow glass microspheres coated with one or more materials. Measurement of the thickness and uniformity of these targets is an important part of ICF experiments.

Previous reports have discussed the use of optical interference microscopy to measure thickness and uniformity of glass microsphere targets.<sup>1,2</sup> In this report we describe how similar techniques are used to measure thickness, index of refraction and uniformity of multilayer films and coatings. We discuss procedures for manipulating and examining microsphere targets to measure surface defects and wall thickness variations anywhere on the target. Finally, we describe the measurement of the individual components and final assembled structure of double-shell fusion targets.

### Thickness and Refractive Index Measurements

Interferometric measurements of fusion targets can be made with any of a number of different interference microscopes. We will describe our measurements with reference to the double pass Twyman-Green interference microscope shown schematically in Fig. 1, which has proven versatile and convenient. We use both white light and a monochromatic source with a wavelength of  $0.535 \mu\text{m}$ . Because our interferometer is double pass, a shift of one fringe corresponds to a change in optical path of  $0.268 \mu\text{m}$ .

Figure 2 illustrates the measurement of thickness and index of refraction of a transparent film. Using a white light interference pattern as a reference, we can measure the difference between the optical path to the top surface of the film,  $P_0$ , the path to the substrate surface,  $P_1$ , and the path to the substrate through the film,  $P_2$ . These optical path differences are related to the film thickness,  $t$ , and refractive index,  $n$ , by:

$$P_1 - P_0 = t \quad (1)$$

and

$$P_2 - P_0 = nt \quad (2)$$

We obtain the thickness uniformity and surface roughness of the film by measuring the uniformity of the fringe pattern at each interface. This procedure applies equally well to measuring the thickness and surface smoothness of a nontransparent film.

We use a similar technique for measuring a multilayer coating on either a flat substrate or a microsphere. As long as there is a refractive index change of about 0.05 or greater between the layers, enough light will be reflected from the interface to allow us to locate it. Figure 3 illustrates this measurement for a multilayered coating on a microsphere. For each layer of thickness  $t_i$  and index of refraction

$n_i$ , the optical path through the layer is  $n_i t_i$ . If only the optical path to each interface can be measured, we must know the index of refraction of each layer to calculate the thickness. If in addition we measure the optical path through the entire sphere, we can determine one unknown refractive index. Measurement of a multilayered coating on a flat substrate is made in exactly the same way. In this case measurement of the total film thickness at an edge again allows us to determine one index of refraction.

The optical path differences described above can be measured several ways. If the layer is thin enough that both surfaces are in focus simultaneously (up to 20 - 30  $\mu\text{m}$  for an objective of moderate magnification), then a calibrated optical path compensator can be used to vary the pathlength of one arm of the interferometer as we locate the white light fringe pattern at each interface. For thicker layers we must move the sample relative to the optics. In this case a mechanical probe or laser interferometer is used to measure the change in optical path. (In either case one can always resort to counting fringes under monochromatic illumination.)

The accuracy of these measurements is generally limited by our ability to locate the center of the white light fringe pattern. For measuring the height of a step (as in Fig. 1) or the thickness of a sample less than about 5  $\mu\text{m}$  thick, the center of the fringe pattern can be determined to about 1/10 fringe or 0.03  $\mu\text{m}$ .

For thicker films and for measuring the location of weakly reflecting interfaces, the accuracy is limited by the effects of dispersion in the material,<sup>3</sup> phase changes on reflection, and the difficulty of locating the center of a weak interference pattern. These effects limit the accuracy to about  $\pm 1 - 2$  fringes ( $0.3 - 0.5 \mu\text{m}$ ).

Film uniformity is measured to  $0.03 \mu\text{m}$  even for thick layers since relative variations of  $1/10$  fringe are fairly easy to observe. The index of refraction measurement accuracy depends on the thickness of the material, and is about  $0.01$  for a  $5 \mu\text{m}$  thick sample.

#### Total Surface Inspection and Uniformity Measurements for Target Spheres

The exacting specification for ICF targets require that we inspect the entire surface of the sphere for defects and measure the uniformity of the wall thickness from point to point. For these measurements we have coupled a modified version of the Twyman-Green interference microscope with a microsphere manipulation system which allows us to systematically inspect the entire target.<sup>4</sup> Figure 4 illustrates how this system operates. The target is held between two flat manipulating tips, the motion of which is controlled by a microprocessor. The tips are moved equal distances in opposite directions, causing the target to roll about its center without displacement. Two perpendicular directions of rotation allow us to place the target in any desired orientation.

For surface measurements the operator can scan the target for contamination using the interferometer as an ordinary microscope. He can also use the system in a reflection interference mode to measure surface defects. In this mode the system is very sensitive to motor vibration and the manipulator must be stopped while a measurement is made.

The most useful application of this system is for measuring wall thickness uniformity. As the microsphere is rotated, the operator views the interference pattern formed by light passing through the target. Thickness changes appear as shifts in the fringe pattern.

When measuring wall thickness defects in this way, we divide the defects into the three types illustrated in Figure 5. The first type is one in which both the inner and outer surface of the target are spherical, but they are not centered with respect to each other. In this case the wall thickness variation with angle is approximately:

$$t(\theta) = t_0 + \Delta t_1 \cos \theta. \quad (3)$$

The second defect type is one in which either the inner or the outer surface of the target is slightly elliptical. In this case the wall thickness is approximately:

$$t(\theta) = t_0 + \Delta t_2 \cos 2\theta. \quad (4)$$

We refer to these two defect types as  $\lambda = 1$  and  $\lambda = 2$ , respectively, considering them as the first two terms in a Fourier expansion. The third type of defect is a localized thick or thin area. (We consider "localized" to mean covering an angle of less than about  $90^\circ$  on the target.)

There are a number of reasons for choosing this division of the defects. First, any wall thickness variation can be approximated as a combination of these defects. Second, each of these defects appears in a very characteristic way when seen in the interference microscope and manipulation system. Third, these defects are closely related to the spherical harmonic decomposition components which are important when analyzing the fluid instability behavior of the target as it is imploded.<sup>5</sup>

Describing the measurement of these wall thickness defects is easiest if we begin with the local defects. These defects cause a local change in the optical path through the target. As the defect passes across the center of the field of view the operator observes the fringe shift caused by the defect. The change in optical path,  $\Delta P_L$ , is related to the change in thickness,  $\Delta t_L$ , by

$$\Delta t_L = \frac{\Delta P}{(n-1)} \quad (5)$$



Measurement of  $\lambda = 2$  defects is similar to measurement of local defects. As the target is rotated, the fringe pattern appears to have a "breathing" motion, alternately emerging from the center of the sphere and disappearing into it as we scan across the thick and thin areas. The magnitude of the defect,  $\Delta t_2$ , is given by

$$\Delta t_2 = \frac{\Delta P_2}{4(n-1)} \quad (6)$$

where  $\Delta P_2$  is the total difference in optical path between the thickest and thinnest paths through the sphere.

Measurement of  $\lambda = 1$  defects is somewhat more complicated, and a detailed explanation is given elsewhere.<sup>2</sup> A key point is that to accurately measure  $\lambda = 1$  defects the target must be oriented so the defect axis is perpendicular to the optic axis of the microscope. With the manipulation system we can do this rapidly and precisely.

One drawback of these measurements is that for the  $\lambda = 1$  and  $\lambda = 2$  defects we cannot tell which target layer contains the defect. At present this is not a serious problem, as in most cases any defect makes the target unusable. All of our present transparent target materials have a refractive index between 1.4 and 1.7, so we can use a median value to approximate the defect thickness.

For complete specification of the wall thickness variations it is necessary to measure both the magnitude and relative orientation of the  $\lambda = 1$  and  $\lambda = 2$  defects. In practice this is rarely done. What we are usually interested in is the maximum variation in wall thickness of the sphere. If the axes of the two defects are aligned with each other, the maximum deviation from the average wall thickness is simply the sum of the two defects. If the defect axes are misaligned, the maximum deviation is reduced somewhat, but is always greater than 85% of the sum of the two defect amplitudes. In practice we therefore simply measure the magnitude of each defect, ignore the relative orientation, and approximate the wall thickness variation as the sum of the two. Any local defects are measured individually and cataloged.

#### Double-Shell Target Measurement

A third application of interference microscopy to ICF target fabrication is in the assembly of double-shell targets.<sup>6</sup> Present versions of these targets are made by assembling two polystyrene hemispheres around an inner microsphere containing the DT fuel. We make a number of measurements to assure the quality of the individual target parts and of the final assembly.

Typically spheres for these targets must have no overall wall thickness variations larger than  $0.5 \mu\text{m}$ , and local defects must be less than  $0.3 \mu\text{m}$  in amplitude. Each sphere is measured in the interferometer

and manipulation system described above to assure that these requirements are met. The hemispheres for the outer shell must also meet strict specifications. Thickness variations must not exceed about 2% and, to assure accurate assembly, the rim must be flat within  $0.5 \mu\text{m}$ . We measure thickness variations by holding the hemisphere on a tiny vacuum chuck and rotating it in the field of view of the interference microscope. We measure the flatness of the hemisphere rim by observing the interference pattern on this surface as shown in Fig. 6.

The inner sphere, which is held between two thin polymer films, must be centered to an accuracy of  $2 \mu\text{m}$ . We make two interferometric measurements which help achieve this. First we measure the centering of the microsphere between the polymer films by measuring the distance from the top of the inner microsphere to the polymer film on both sides of the sandwich as shown in Fig. 7 a. After the target is assembled, we measure the centering of the inner sphere by measuring the gap between the outer and inner shell at several points around the assembly (Fig. 7 b). These centering measurements are a good example of a case in which either the interferometer optics or the sample must be moved to locate the interfaces. As with thick layers, these measurements have an accuracy of about  $0.3 \mu\text{m}$ .

Summary

We have developed interferometric techniques for measuring a variety of films and microspheres used as laser fusion targets. We are able to measure the thickness and uniformity of single and multilayered targets, the index of refraction of a single layer, and the components and centering of double shell targets. The accuracy of these measurements is about 0.03 to 0.5  $\mu\text{m}$ , depending on the specific application. These techniques are rapid, accurate and nondestructive and are used for most measurements of inertial fusion targets made with transparent materials.

## NOTICE

This report was prepared as an account of work sponsored by the United States Government. Neither the United States nor the United States Department of Energy, nor any of their employees, nor any of their contractors, subcontractors, or their employees, makes any warranty, express or implied, or assumes any legal liability or responsibility for the accuracy, completeness or usefulness of any information, apparatus, product or process disclosed, or represents that its use would not infringe privately-owned rights.

Reference to a company or product name does not imply approval or recommendation of the product by the University of California or the U.S. Department of Energy to the exclusion of others that may be suitable.

References

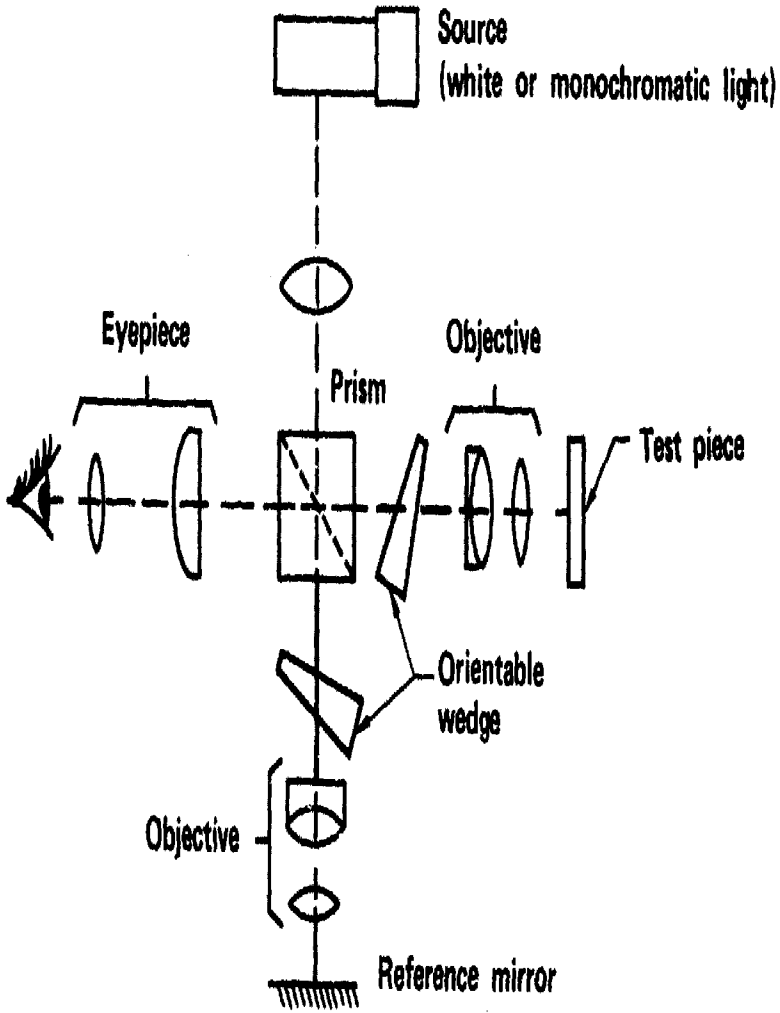
1. Berthold W. Weinstein, J. Appl. Phys. 46, 5305 (1975).
2. B. W. Weinstein and C. D. Hendricks, Appl. Opt. 17, 3641 (1978).
3. Jeffrey A. Tarvin, Appl. Opt. 18, 3213 (1979).
4. B. W. Weinstein, C. D. Hendricks, C. M. Ward and D. L. Willenborg, Rev. Sci. Instrum. 49, 870 (1978).
5. J. D. Lindl and W. C. Mead, Phys. Rev. Lett. 34, 1273 (1975).
6. C. W. Hatcher, L. E. Lorensen and B. W. Weinstein, "Double Shell Inertial Confinement Fusion Target Fabrication," J. Vac. Sci. Technol. (In Press).

Figure Captions

1. Tyman-Green interference microscope used for fusion target measurement.
2. Measurement of the thickness and index of refraction of a transparent film. We use a white light interference pattern as a reference to measure the difference between the 3 optical paths.
3. Measurement of a multi-layer film. Even for small refractive index changes between layers, enough light is reflected from each interface to form an interference pattern which we can use to locate the interface. The optical path through each layer is  $t_i n_i$ .
4. a) Schematic diagram of the interference microscope and microsphere manipulator used for inspecting a target sphere in all orientations.  
b) The transmission interference pattern seen on a target in the manipulator.
5. We classify wall thickness defects as  $\epsilon = 1$  or nonconcentricity as shown in (a),  $\epsilon = 2$  shown in (b), or as a local defect, also shown in (b). The defect magnitudes are  $\Delta t_1$ ,  $\Delta t_2$  and  $\Delta t_L$  respectively.

6. Interference pattern on the rim of a polystyrene hemisphere used for the outer shell of a double-shell target. Machining marks show about  $0.01 \mu\text{m}$  (1/3 fringe) variations. The inner edge is raised about  $0.3 \mu\text{m}$  (1 fringe).
  
7. Measurement of the centering of double-shell targets. The centering of the inner sphere between the support films is checked prior to assembly as shown in (a). After assembly the gap between the inner and outer shell is measured at several points on the target as shown in (b).

# INTERFERENCE MICROSCOPE SCHEMATIC



10-10-1078-3844

8/80

Fig. 1



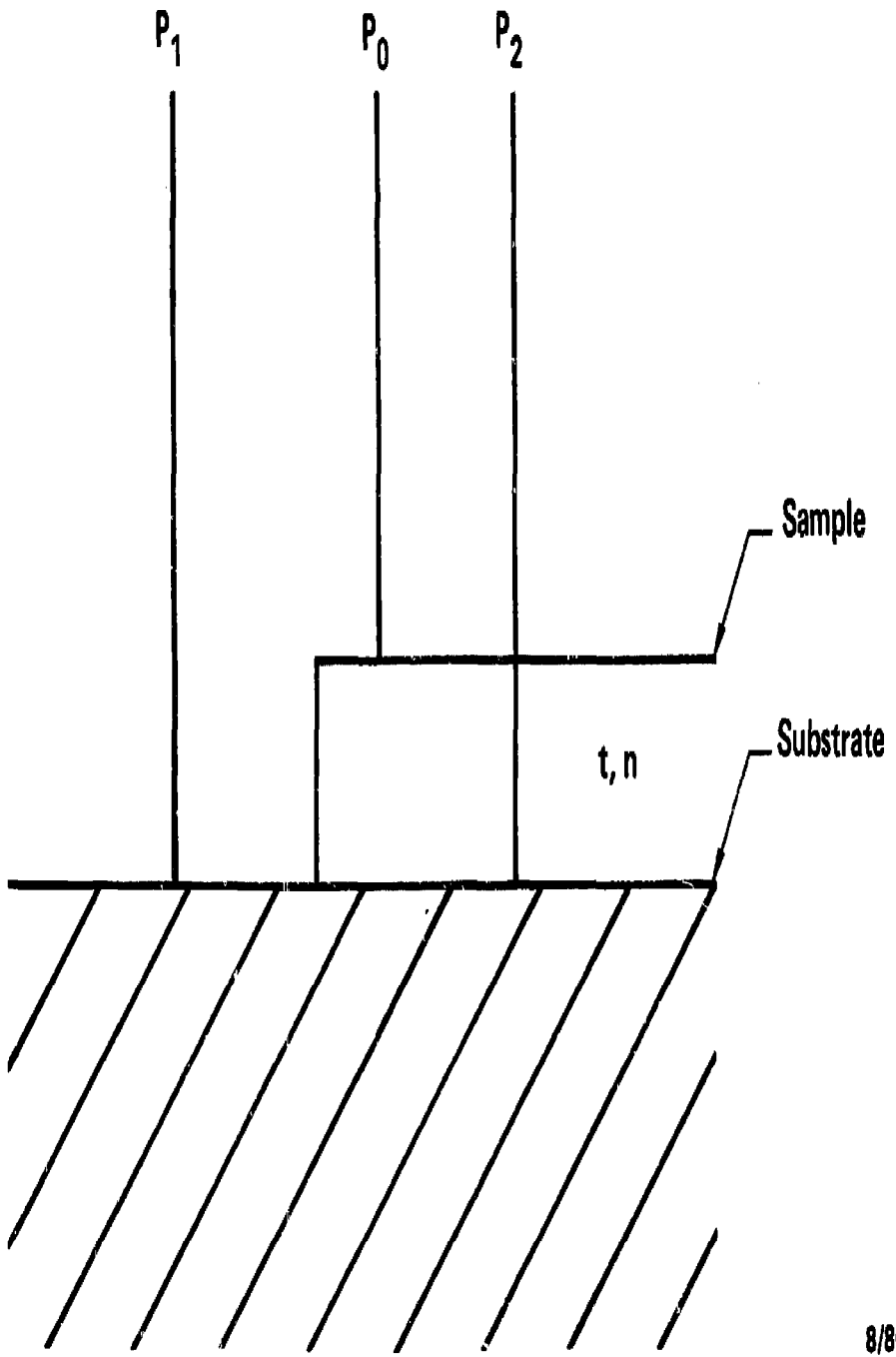


Fig. 2

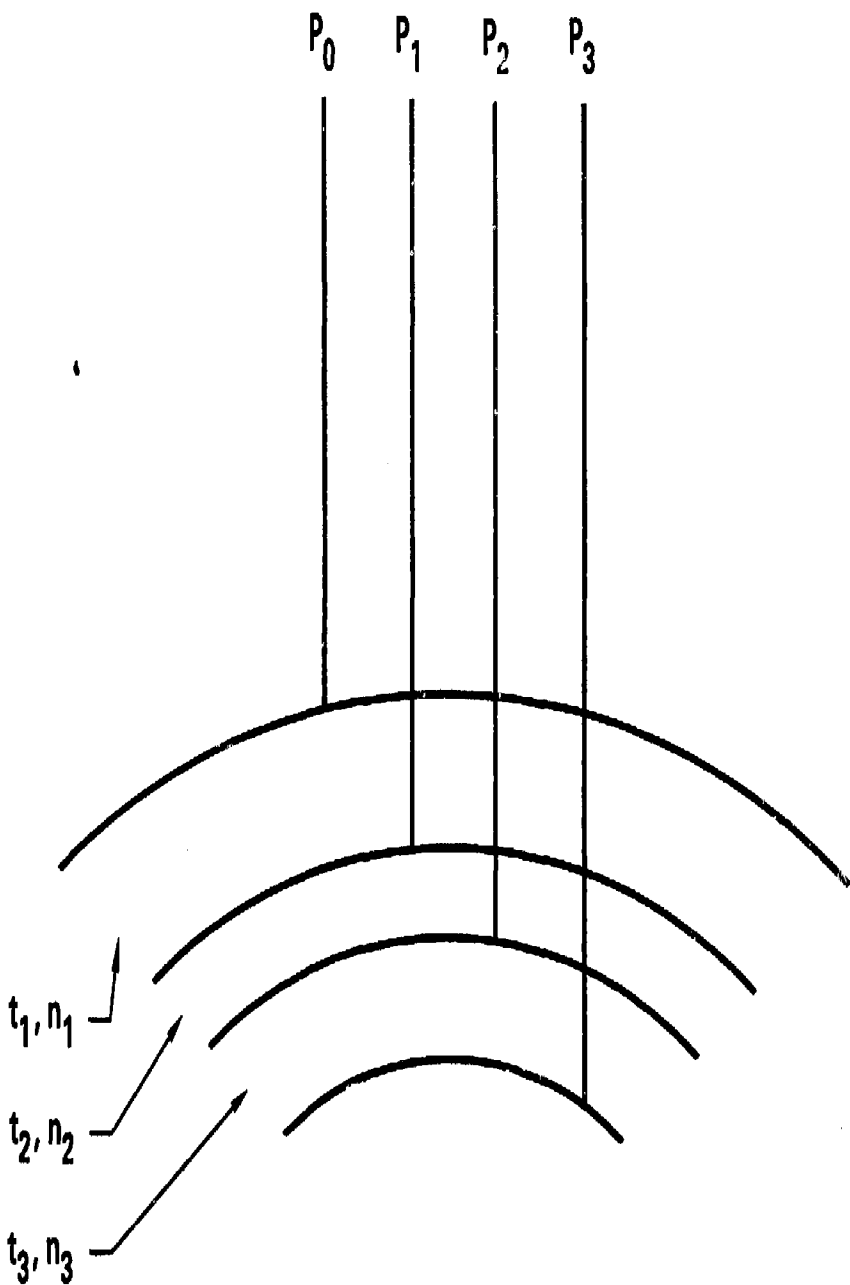
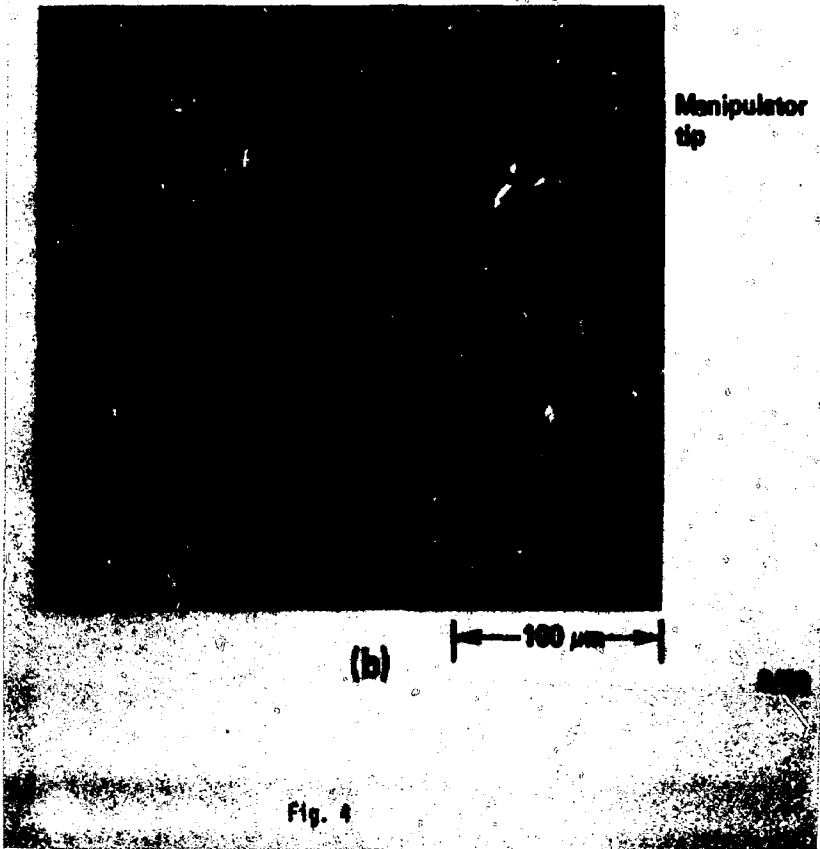
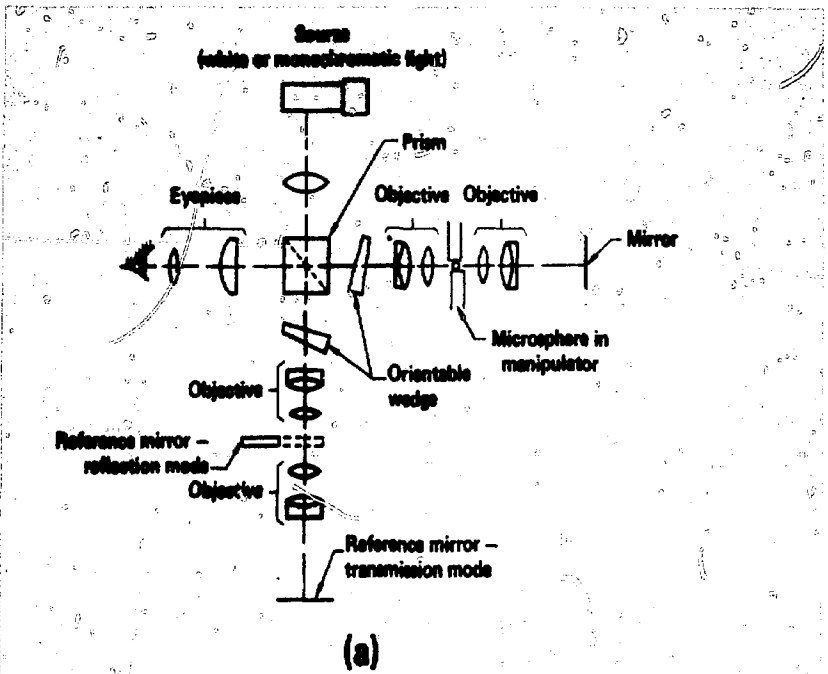
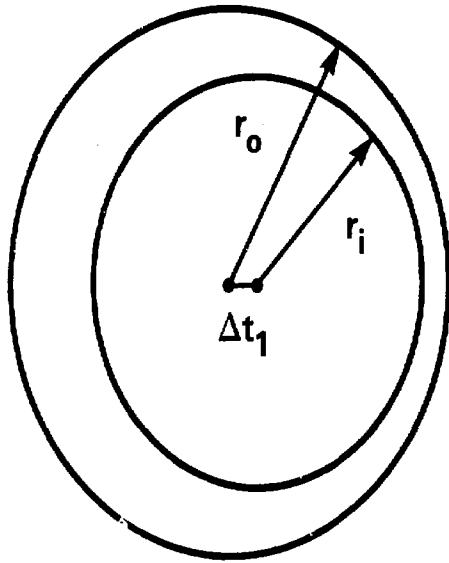
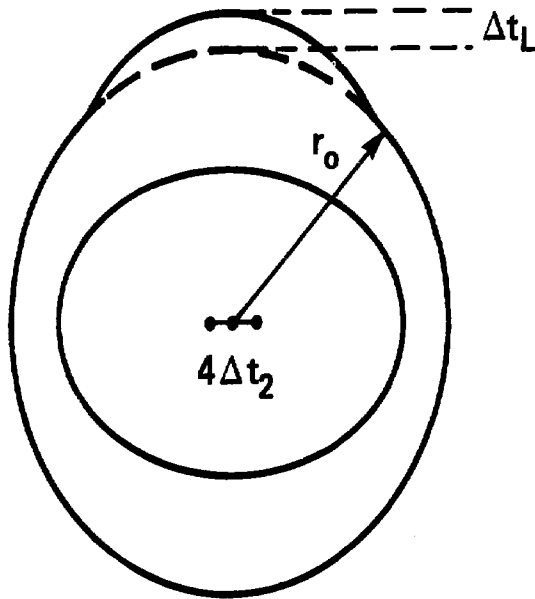


Fig. 3



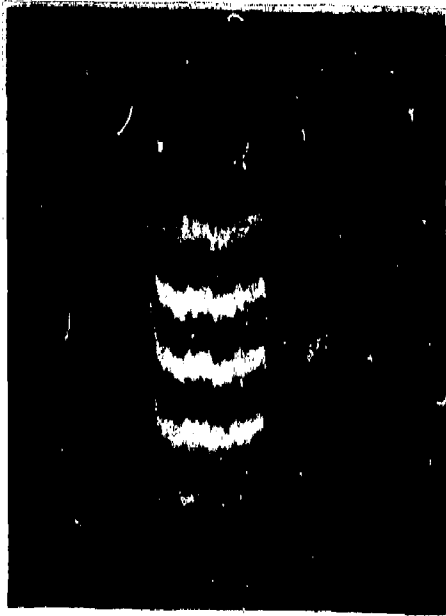


(a)



(b)

Fig. 5



50  $\mu\text{m}$

Fig. 6

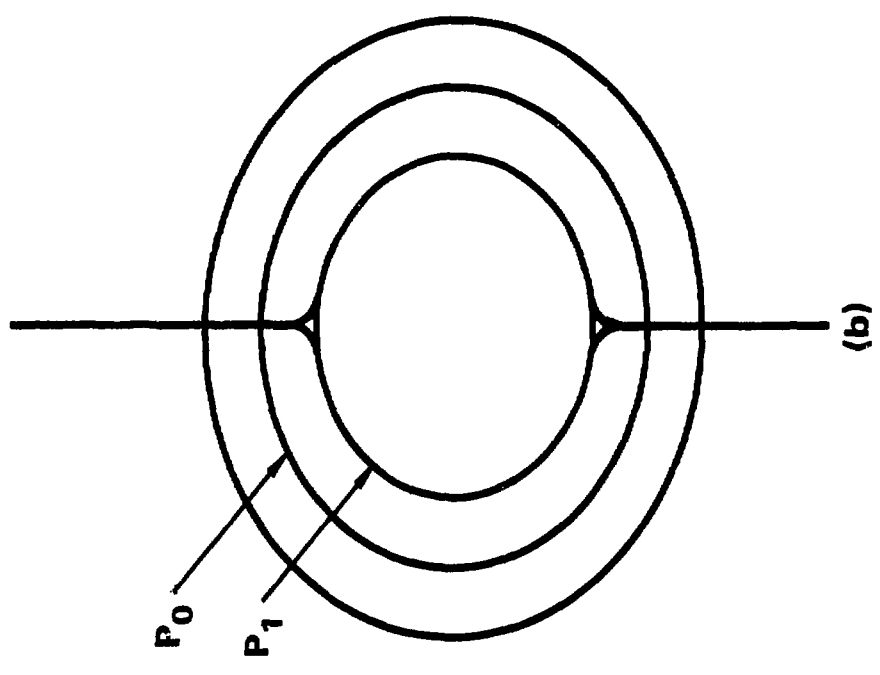
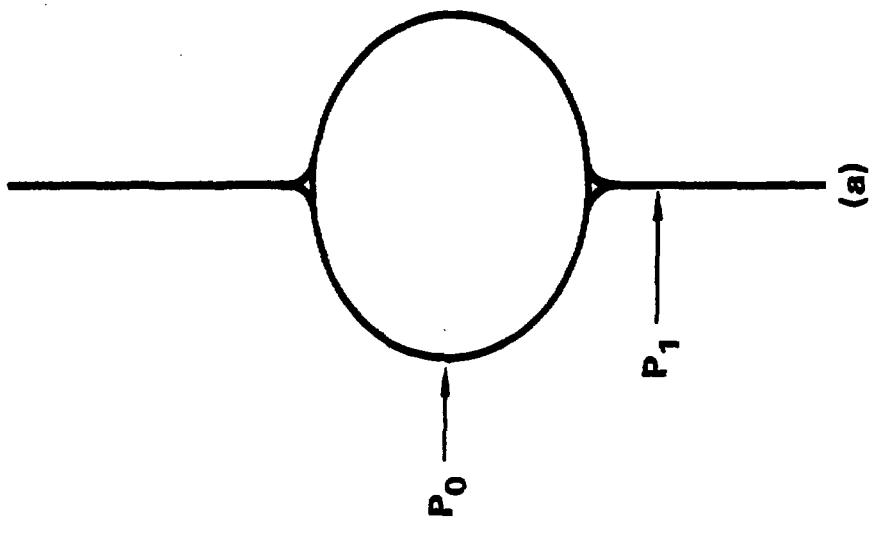


Fig. 7